Optical representation of sound fields with phase and amplitude recording

Schroeder, H. J.

Publisher's version / Version de l'éditeur:
https://doi.org/10.4224/20331423
Technical Translation (National Research Council of Canada); no. NRC-TT-1258, 1966

PREFACE

It is frequently necessary in acoustical measurements to be able to plot the pressure sound field in terms of isobars (curves of equal pressure). Normally this is done by tediously recording pressure levels in the space in question, searching for points of equal pressure, then joining them with a curve. The author of this paper describes a method in which the contours in a plane are recorded automatically by using the electrical output of a microphone to modulate a light source, then photographing it. The amplitudes in a given plane are picked off in 5 db contours.

This is a useful method for plotting contours of standing waves, e.g. in a resonant enclosure. The author goes further and shows that it is also possible to represent progressive waves. To do this a phase detector is included in the receiving system and the phase of the received signal is compared to that of the source. This undoubtedly finds applications in measurements made in free space or anechoic chambers, e.g. in the pattern produced by scattering objects or the directivity patterns of sound sources. Finally, the author, after showing how the technique works for simple sources, considers more exotic examples such as bells and violins.

The Division of Building Research wishes to record its gratitude to Mr. D.A. Sinclair, Head, Translations Section, National Research Council, for translating this paper and to Dr. R.J. Donato of this Division who checked the translation.

Ottawa
September 1966

R.F. Legget
Director

NATIONAL RESEARCH COUNCIL OF CANADA

Technical Translation 1258

Title: The optical representation of sound fields with phase and amplitude recording
(Optische Schallfelddarstellung mit Phasen- und Amplitudenaufzeichnung)

Author: H.-J. Schroeder

Reference: Acustica, 13 (2): 92-103, 1963

Translator: D.A. Sinclair, Translations Section, National Science Library

THE OPTICAL REPRESENTATION OF SOUND FIELDS WITH PHASE AND AMPLITUDE RECORDING

Abstract

The construction and mode of operation of an apparatus are described, which permits the optical representation of stationary sound fields in air. From the method proposed by Kock and Harvey for the optical representation of progressive waves a new method has been developed, which permits also the recording of isobars of the sound pressure. The sound pressure pattern of a sound field is now represented by six isobars with a level difference of 5 db. This method is applied to the fields of various sound sources, a spherical radiator, a group of two single radiators, a bell, a cylindrical tube and a violin.

1. Introduction

Practically speaking there is only one method of representing sound fields in air optically, namely by scanning with a probe microphone. The acoustical process is thereby converted into an optical one which is imaged at the probe aperture. The image is produced as a result of the microphone and lamps scanning a plane of the sound field in a darkened space. This process is photographed (Fig. 1).

In 1950 Kock and Harvey[1] reported the visualization of sound waves and electromagnetic waves in the centimetre region. Chiefly emphasized was the representation of progressive waves. This kind of representation is obtained when a phase-locked comparison voltage is superimposed on the voltage generated at the microphone, and the total voltage is used to control the lamp. The resulting image is more or less an instantaneous picture of the sound field.

The amplitude distribution in the field was represented by the fact that the brightness of the lamp was controlled by the sound pressure. Thus a picture is obtained in which regions of high sound pressure appear bright. However, this method is not very suitable for quantitative evaluation, which is extremely complicated at best (evaluation by the grey scale).

In recent years several authors[2-5] have dealt with Kock and Harvey's method without finding a satisfactory solution to the amplitude recording problem. The present paper offers a new possibility of accurate representation of the sound field with respect to phase and amplitude[6]. The uncertainty of recording is less than 1 cm, the level uncertainty in the drawing of the isobars, less than 0.3 db. Field segments of approximately 1 m^2 can be photographed.

2. The Construction of the Measuring Apparatus

2.1. Mechanical part

The mechanical part of the apparatus comprises the device for scanning the sound field. Its purpose is to guide the lamp and the microphone through the sound field along the desired path. Spiral-shaped scanning paths are employed. For purposes of photographic recording the distance between two consecutive raster lines must be constant and less than the light exit aperture. This prevents any unexposed strips from appearing on the film between lines. The distance between consecutive spiral paths must be small enough so that no interfering lines appear on the sound field picture. The distance between lines must also be adapted to the "acoustic resolving power" depending on the dimensions of the microphone probe.

The apparatus is constructed as follows (Fig. 2).

A pipe 30 mm in diameter and about 3 m long rotates about a horizontal axis. On this pipe is mounted a slide which can move parallel to the axis of the pipe, but cannot rotate about the pipe axis. On one end of the slide the microphone is mounted, so that when the slide is stationary it describes a circle in a vertical plane. A rack is mounted on the slide which engages with a pinion. The latter is controlled so that the slide moves 2.7 mm along the pipe every revolution. As a consequence, the microphone follows a spiral path.

The driving mechanism is designed to keep the scanning speed constant. The exposure of the film thus depends exclusively on the brightness of the lamp. (For constant intensity of the light, a change in the scanning speed would affect the exposure time). The upper speed limit is given by the development of wind noises and interferences due to the Doppler effect.

For automatic control of the rpm a continuously variable speed transmission is employed. The microphone speed is 1.3 m per second and is kept constant to approximately ±10%.

2.2. Acoustic-electric part

The microphone must meet the following requirements:

1. Its directional characteristic must, as far as possible, be spherical.
2. Sound field distortions due to the microphone must be kept as small as possible.
3. The microphone must show sufficient sensitivity.

Putting the upper limiting frequency at 15 kc, we get an estimated permissible dimension d of the microphone (in order to satisfy requirements

1 and 2) of

$$d < \frac{\lambda_{15\ kc}}{2}, \qquad (1)$$

and on account of $\lambda_{15\ kc} = 2.2$ cm:

$$d < 1.1 \text{ cm}.$$

More suitable than the use of such a microphone is the use of a probe microphone. In this case only the probe needs to be dimensioned according to the requirements. From the acoustical standpoint, the length of the probe shound be as great as possible, in order to keep disturbances of the sound field due to nearby parts of the rotary framework small. On the other hand, the diameter of a probe must be kept as small as possible in order to avoid sound field distortions due to the probe itself and to get a spherical characteristic for high frequencies. Neither requirement can be fully realized because the pipe damping would be too great.

The dimensions of the probe, accordingly, should be so chosen as just to ensure realization of points 1 and 2 for the limiting frequency.

The probe was designed to have a length of about 750 mm, an inside diameter of 8 mm and an outside diameter of 10 mm. For f = 15 kc (λ = 2.2 cm) a pipe damping of approximately 6 db is obtained.

The directional characteristic of the probe can be determined approximately by obtaining the directional factor of a circular piston membrane, the diameter d of which is equal to the inside diameter of the pipe:

$$\underline{R}^{*} = 2\ \frac{J_1\left(\frac{\pi d}{\lambda}\sin\gamma\right)}{\frac{2\pi d}{\lambda}\sin\gamma},$$

$$\underline{R} = 2\,\frac{J_1(x)}{x} \text{ for } x = \frac{\pi d}{\lambda}\sin\gamma. \qquad (2)$$

where $J_1(x)$ is the Bessel function of first order, γ is the angle of direction, forming the corresponding straight line projection with the z axis. The system of coordinates is so chosen that the z axis coincides with the pipe axis, and the opening of the pipe lies in the x, y plane. The principal axis is then situated at $\gamma = 0°$, i.e. in the direction of the z axis.

In the test set-up, the tip of the probe is situated in the x, y plane. The test object can be situated either in the x, y plane, or in front of it. In the former case the field is photographed only in the one direction of propagation which is of interest (for instance loud-speaker records). In

---

* Translator's note: An underlined symbol signifies gothic typescript in the original.

this case γ is always 90°, and the directional characteristic, on account of the rotational symmetry of the probe, plays no part. However, if the test object is situated in front of the x, y plane, as is often the case, then γ may be anywhere between 0 and 90°.

For $\gamma = 90°$, $\sin \gamma = 1$ and $f = 15$ kc, $\lambda_{15\ kc} = 2.2$ cm for $d = 0.8$ cm gives a ratio of

$$\frac{d}{\lambda} = \frac{0.8}{2.2} = \frac{1}{2.8} . \tag{3}$$

Thus

$$x = \frac{\pi d}{\lambda} \sin \gamma, \tag{4}$$

$$x = \frac{\pi 0.8}{2.2} = 1.12 \text{ and}$$

$$\underline{R} = \frac{2J_1(x)}{x} \approx 0.8. \tag{5}$$

Since for $\gamma = 0°$ $\underline{R} = 1$, the departure from the spherical characteristic is

$$20 \log \frac{0.8}{1} = -2 \text{ db}. \tag{6}$$

This is the least favourable case possible.

To sum up, we may say that up to $f = 10$ kc the requirement of a spherical characteristic is practically satisfied. For $f > 10$ kc an error arises which can be reduced either by reducing the diameter of the probe, or by avoiding a very large angle.

2.3. Electronic part

The signal from the microphone is fed to a preamplifier (Fig. 3). Despite careful atmospheric and vibration insulation of the drive mechanisms, interferences get to the microphone and these must first be removed. The high pass filter, primarily, serves this purpose, because the interference level components from the motor contain predominatly low frequencies. Additional filtration is carried out with the aid of a third order filter.

What is the form of the useful voltage when the source emits a sinusoidal sound? On passing through the sound field a signal is received which is amplitude, frequency and phase modulated. The amplitude modulation arises from the fact that the receiver is moving through regions of different sound pressure. The modulation frequency is comparatively low. It depends on the sound field structure and the scanning speed. The phase

and frequency modulations are due to the fact that the distance between the microphone and the stationary sound source is continually changing in the course of the scanning process (Doppler effect).

The amplitude and phase modulations are used to control the light source. The frequency modulation is not evaluated as such. At the maximum it can only be 0.4% and would be a disturbing factor only if very narrow band filters were employed.

2.3.1. Phase channel

The phase modulated signal is used to represent the progressive wave in the sound field, much as in the manner suggested by Kock and Harvey[1].

At distances $r = \lambda, 2\lambda, 3\lambda, \ldots$ similar phase conditions prevail. When we consider the phase angle between the generator voltage which feeds the sound source and which may serve as a comparison voltage, and the microphone voltage, then the phase rotates 2π as the microphone moves a distance λ away from or towards the source. This fact is used to represent the progressive wave by superimposing the microphone voltage on a phase-locked comparison voltage. The total voltage is used to modulate the lamp current. In order to obtain a degree of modulation which is independent of the microphone distance, the value of the microphone voltage must be kept constant with the aid of a limiter. In general, the generator voltage can be used for comparison purposes. However, it is equally possible to use the output voltage of a second microphone in a fixed position.

The manner of operation of the phase channel is indicated in Fig. 4. The oscillogram shows the conversion of the microphone voltage (at the top of the picture) into the lamp current (below). In scanning the sound field a segment was chosen in which the microphone was moving towards a point sound source and then moving away from it again. The frequency was 4 kc. It will be noted that the modulation of the lamp current is largely independent of the microphone voltage.

2.3.2. Amplitude channel

In order to extend the earlier type of representation of the progressive wave, an apparatus was developed which makes possible the visualization of isobars (lines of equal sound pressure), so that besides the phase relation, the amplitude distribution can also be made visible. For this purpose the amplified and filtered microphone voltage is rectified and fed to a voltage divider (Fig. 3). The latter has 5 tap stages, delivering incremental voltages U_1 to U_6 in 5-db intervals. Each of these voltages controls a voltage discriminator (Schmitt-Trigger). If the voltage goes either above or below the latter's threshold voltage, a positive or negative impulse, as

the case may be, is obtained as an output voltage. The outputs of the six discriminators are connected in parallel. This apparatus operates as follows:

As the microphone voltage increases, the largest of the tapped voltages (U_1) reaches the response value of the corresponding discriminator 1, which then delivers an impulse. When the sound level at the probe tip has risen by 5 db, the second largest voltage U_2 will have just reached the value necessary in order to produce a response of discriminator 2. The impulse 2 appears at its output. As the sound level continues to rise voltages U_3 to U_6 in turn reach the trigger voltage of their discriminators, so that in each case an impulse is emitted at intervals of 5 db. The same thing occurs as the level drops: the individual voltages control their discriminators in the reverse output state, thus generating impulses for the opposite direction.

The impulses are then used to control the lamp. In this manner pulses of light are produced as the sound level goes above or below certain defined levels. Curves of equal sound pressure are produced on the film from these pulses of light.

The discriminators were adjusted so that the hysteresis would be as small as possible[7].

The hysteresis itself guarantees that the Schmitt discriminator will operate in a stable manner. It is possible, of course, to make it very small, but then a danger arises that even a very slight disturbance of the input voltage would result in an unintentional reversal. Moreover, another result of reducing the hysteresis is that the anode voltage jumps become smaller and smaller, and finally reach 0. On the other hand, by suitable selection of tubes and of the correct operating point, the hysteresis can be reduced without the above-mentioned disturbing properties. The circuit was chosen so that the hysteresis would be less than 100 mv for a response voltage of 2.5 v. The resulting error is less than ±4% or ±0.3 db. We shall have more to say below about the effects of this.

The change of response level during the exposure time is less than 0.05 db, and is thus negligible.

The pulses are formed by differentiation of the anode voltage jumps.

We now get a diagram in which the sound field would be characterized by lines of equal sound pressure. However, it would be impossible to distinguish whether a given line, which owing to an equal impulse level produces equal blackening of the film, would represent an isobar of higher or lower sound level than the adjacent line. For this reason the impulse level of the discriminator output voltage was varied in such a way that the output pulse of the first discriminator, which responds to the smallest voltage and hence generates the 0 db isobar, receives the lowest impulse level. In the positive of the sound field photograph this corresponds to a thin and narrow

line. The pulses of the remaining discriminators are staged in such a way that discriminator 6, which generates the 25 db isobar, has the greatest amplitude, which in turn modulates the maximum permissible lamp current and thus traces the brightest and thickest line.

Figure 5 shows an oscillogram which gives the microphone voltage at the top and the lamp current in amplitude representation below. The staging of the pulse levels is clearly recognizable. At the right and at the left of the photograph it will be seen that some impulses come in rapid succession and some overlap. This is because the decrease of microphone voltage at comparatively great distance does not occur continuously owing to reflections. The fact that the impulses are not symmetrical with respect to the peak of the microphone voltage will be discussed below in greater detail in connection with the diagram errors.

The available bits of information (impulses of the amplitude channel, the filtered and amplified microphone voltage, and the phase-locked comparison voltage) are suitably mixed and amplified in mixing and output amplifiers, and are fed to the lamp.

2.4. Electrical-optical part

The signals, which flow through the output tube in the form of impulses and pulsating direct current, must be converted into an equivalent light beam. The lamp must meet various requirements, of which the most important are the following:

1. The lamp must be subject to modulation of its brightness with little inertia. By little inertia, we mean here that every detail of the sound field structure should be imaged without distortion at a scanning speed of approximately 1.3 m/s. In converting the pulses, the aim must be to have a pulse recorded as a point, with the result that a thin line will appear in the figure when the points are put together. The luminous duration should therefore be such that during the movement of the lamp it will illuminate a path only of approximately 1 mm. Referred to the time, this means that a light pulse of approximately 0.8 ms duration must be produced. The top limiting frequency must therefore be greater than 1 kc.

   This eliminates all incandescent lamps, even those that are preheated and have very thin filaments.

2. The second requirement relates to susceptibility to modulation. The light source must have as great as possible a range of modulation. Between the two boundaries given by the permissible load or acceptable overload (100% modulation) and the unloaded state (modulation 0%), there must be a constant relationship between current or voltage on the one hand and the

light intensity on the other.

3. The light intensity of the lamp must be great enough so that even after taking all losses into account the illumination intensity on the photographic film is sufficiently great to produce adequate blackening.
4. The light source must be point shaped and be as small as possible, since it must be situated in the vicinity of the sound field that is being scanned.

Requirements 1 - 3 are met by the Osram 767740 point source glow lamp. The lamp is l = 80 mm long, with a diameter of d = 25 mm. With these dimensions it is impossible to mount the lamp on the tip of the probe. A secondary emitter must therefore be provided.

2.5. Photographic recording and imaging errors

From the photographic point of view, the aim is to get a light distribution curve of the emitter which will ensure a uniform exposure of the film in relation to the solid angle.

Accordingly, therefore, the light beam should be guided so that the divergent radiation from the lamp is at first collected, is conducted parallel to the probe as far as the tip, and then strikes the secondary emitter, which provides for the desired distribution in space. For the emitter a small plane-convex lens about 8 mm in diameter is used, with the surface of the plane side roughened so as to act as a ground glass screen and cause additional scattering.

This light beam conversion is not very efficient. Therefore maximum photographic sensitivity, i.e. a fast objective and film material of the highest sensitivity, must be used. We employed Agfa Rekord film, which can be pushed to about 36/10 DIN.

The lag between the acoustical measurement at the probe tip and the optical signal causes a distortion equal to the distance through which the microphone and lamp have moved in the same period.

The lag Δt is about 10 ms, and comprises the time taken by the sound to traverse the probe, the time taken to initiate the filters, and the time constant of the rectifier circuit. Added to this is the hysteresis error in the amplitude representation, which acts as an apparent lag.

The resulting imaging error can be eliminated in a simple manner, by displacing the position of the optical image (the ground glass plane at the tip of the probe) a distance corresponding to the lag time (about 13 mm). The light signal is then recorded at the position at which the probe axis was situated 10 ms earlier.

This assumes, of course, that Δt is constant, a condition that applies only to the phase representation. The error which arises in the amplitude representation owing to the hysteresis of the discriminators, is not so easily taken care of. We shall therefore investigate it briefly. As already mentioned, the hysteresis is 0.3 db. For an increasing microphone voltage, the impulse for producing the isobars is only given when the control voltage is +0.3 db above the rated value. In the case of dropping voltage the impulse is generated at -0.3 db. If we again consider Fig. 5, where the microphone voltage, owing to the constant scanning speed and the point form of the sound source follows a symmetrical curve, two facts will be recognized:

1. The hysteresis causes both impulses of a stage to be "too late" by the same amount on account of the symmetry of the voltage curve. As a consequence an additional apparent lag is brought about, which however can be corrected by displacement of the optical image, so that the value of ± 0.3 db for the hysteresis is not identical with the uncertainty involved in the isobar diagram.
2. The magnitude of the apparent lag depends on the steepness of the voltage increase or decrease as the case may be. dU/dr is greatest in the vicinity of the emitter and hence the distortion caused by the hysteresis is smallest here. With increasing distance the steepness decreases and the recording error becomes greater. Assuming a 1/r curve of sound pressure, and drawing the isobars for the maximum level, for example, so that $r_6 = 1.5$ cm, then the isobars of the lowest level will be $r_1 = 27$ cm (-25 db). At this distance the steepness is approximately 0.3 db/cm, with which the displacement attains a value of approximately 1 cm. Theoretically this effect would be recognizable in the sound field pictures, however it has been found that at this distance acoustical disturbances already predominate, as is shown in the next section. In the vicinity of the emitter, however, the error is compensated by the displacement of the optical image.

Nevertheless a slight inaccuracy remains, since the total lag time for the amplitude record is a few milliseconds greater than for the phase record. The distortion, can therefore, amount to a few millimetres, but in most cases this is entirely unimportant, since the discrepancy in the pictures can no longer be recognized.

The optical imaging of a sound field is further supplemented by the superposition of a system of coordinates (grid lines 10 cm apart).

3. Applications

3.1. Sound field records of a spherical emitter

The simplest case is that of omnidirectional emission of the type produced by a spherical emitter of zeroth order. The individual elements of the surface of the sphere here oscillate with constant velocity amplitude, outwards and inwards in phase. The sound field of such an emmiter is characterized by the fact that both the surfaces of equal phase and the surfaces of equal sound pressure amplitude are concentric spheres with the emitter as a common centre. Practically, an emitter of zeroth order in the form of a dilating sphere is unrealizable.

For the tests a miniature magnetic earphone was used which had the following dimensions: diameter 20 mm, height 11 mm and diameter of sound-emitting aperture 2 mm. For the lower frequencies a spherical characteristic is indeed obtained, but the amount radiated is very small.

For sound field representation a section is cut through the field. In the present case the section is best taken through the origin. Owing to the finite dimensions of the emitter, of course, this can not be exactly realized in the present case, but the departures from it are very small. The distance between the emitter and the probe tip of the microphone was about 10 mm.

In the sound field representation the curves of constant phase produce concentric circles whose distance apart is equal to the wavelength. For making the record (Fig. 6) a frequency of $f = 3.4$ kc was chosen. The wavelength is then $\lambda = 10$ cm.

The lines of equal sound level, to be sure, also form concentric circles but their distance apart is not constant. They vary in accordance with the law of propagation. In the spherical wave the sound pressure decreases continuously (even in the near field) at the rate $1/r$. The six isobars are recorded in 5 db stages of the sound level. Denoting the isobars so that isobar 1 is assigned to the relative sound level 0 db, isobar 2 to level 5 db, then isobar 6 corresponds to the largest level $L_6 = 25$ db. In Table I the sound levels L, the sound pressure amplitudes p and the corresponding field point intervals r, as obtained from the $1/r$ law, are given for the six isobars.

Now considering Fig. 7, which shows the sound distribution of the field for the frequency $f = 4.0$ kc, we again see the expected concentric circles in the vicinity of the emitter. With increasing distance, the curves gradually lose their circular shape, and are subject to wavy indentations. In addition, individual islands form between the concentric curves.

These departures from the theoretically expected curve shape at first

strike us as anomalous, but are easy to explain. The space in which the records are being made, although very strongly damped with respect to sound, is not totally free from reflections. Even if it were, some interfering reflections could not be entirely avoided, since the apparatus required for the measurement must be situated in the vicinity of the field to be investigated.

In what follows, the sound field records are to be quantitatively evaluated. It will then be possible to say something about the order of magnitude of the interferences observed. It will be the aim of this evaluation to determine whether the sound emission is spherical. At the given frequency f = 4 kc the ratio $d/\lambda = 1/4.25$ is obtained. With this only a slight departure from the spherical characteristic is expected.

For the evaluation diameters D_1 to D_6 of the recorded isobars are measured. In the case of the no longer circular curves, the extreme values D_{max} and D_{min} are determined. These values are entered in columns 3 and 4 of Table II. The mean values D_{mean} determined from this are given in column 5. With the aid of the 10 cm grid, the scale of reduction M for the diagram is determined. Multiplying the values for D_{mean} by M/2, we get the radii r' in the image plane (column 6). For small radii r' a correction must be applied which takes into account the distance a between the emitter and the tip of the probe. The distance r sought between field points is the hypotenuse of a triangle, the bases of which are the radius r' and the distance a. According to the Pythagorean theorem, then

$$r = \sqrt{a^2 + r'^2} .$$

The distances r between field points thus calculated are entered in column 7. For these points we calculated the sound level values L obtained from the 1/r law. It is best to choose a reference point in the central region, since that will give the most accurate value. For the present example the radius of the isobar 4 was chosen as reference. In column 8 the sound levels $L_{calc.}$ are entered. The difference between $L_{calc.}$ and L is entered as a mean deviation in column 9. Assuming a reading accuracy of ±0.5 mm, then we get the uncertainties given in column 10, referred to the sound level. The waviness of the isobars at a greater distance is a consequence of level fluctuations, which are given in the last column.

Considering the mean errors in column 9, it will be recognized that the latter increase from -0.9 db (isobar 1) to +1.1 db (isobar 6). The drawing of the isobars themselves entails an uncertainty of about ±0.3 db, made up of the error owing to the hysteresis of the discriminators and the calibration of the response voltage. Even when all possible sources of error have been

taken into account, a part of the mean error still remains in the sense that the drop in the level is steeper than given by 1/r. Thus the requirement with respect to the spherical characteristic is not wholly satisfied. The direction of the preferred sound emission is perpendicular to the plane of scanning, or, seen from the position of the earphone, is in the direction of the sound-emission aperture.

The strikingly wavy character of the more distant isobars is a consequence of fluctuations of level amounting to ±0.8 db in the vicinity of isobar 1 and ±0.6 db near isobar 2. In themselves these fluctuations are slight and would scarcely cause any interference for most practical measurement purposes in the sound field. The fact that they appear so prominently in sound field photography lies first of all in the nature of the 1/r decrease and secondly in the exact character of the reproduction method, which shows every detail of the field. In ordinary graphical representation of fields, determined by point-by-point measurement, these fine details cannot be brought out. The same applies to the islands appearing in the pictures.

Since the evaluation showed that for the miniature earphone and a frequency f = 4.0 kc departures from the spherical characteristic were still measurable, an attempt was made to realize the spherical emitter in another manner. For this purpose a thin pipe having an outside diameter of 6 mm and a length of 1 metre was used for sound transmission. A miniature earphone is coupled to one end of the tube while the other end projects as a probe into the sound field. For the frequency f = 4 kc, we thus get a ratio

$$\frac{d}{\lambda} = \frac{0.6}{8.5} = \frac{1}{14.2} .$$

Compared to the first test the value is reduced by 1/3.

Figure 8 shows the sound record of this set-up. The evaluation is carried out in Table III. The mean error lies between 0 and +0.4 db. With an uncertainty of ±0.2 db the level decrease corresponds to the expected 1/r relationship. In comparing this with the sound picture of Fig. 7 it is noted that the departures from the circular shape of the isobars are greater in Fig. 8, as the evaluation (last column, Table III) also indicates. Whereas in Fig. 7 the 4 inner isobars are practically circular, in Fig. 8 only the two innermost are undistorted. The magnitude of the level fluctuation as a function of the distance follows different courses in the two cases. According to Table III (the pipe) we get a fluctuation of ±0.8 to ±0.9 db for isobars 1 to 3, whereas with the miniature earphone the distortion becomes greater with increasing distance. Presumably this effect depends on the fact

that the pipe itself contributes to the sound emission, so that an interference field is formed. Effective insulation of the pipe would result in an increase of diameter, which in turn would increase the ratio d/λ.

For a broad class of experiments in which spherical emitters were needed, therefore, miniature earphones were employed, since these do not cause any additional sound field distortions and satisfy the spherical characteristic requirement approximately.

To conclude these remarks, two additional points may be mentioned:

1. The evaluation of isobars in the immediate vicinity of the emitter is not always possible within the specified uncertainty of measurement. For one thing, the determination of the distance a between emitter and receiver is not always unequivocal, and, for another, we cannot be certain whether in every case the propagation of the sound can be regarded as undistorted, if the microphone probe aperture is very close to the emitter.
2. The isobar curves are as a rule interrupted or broken in two places. This is a minor lack of refinement, due to the following causes:

During the time the microphone is moving along an isobar, i.e. is not intersecting it, the control voltage of the discriminator involved remains constant. If the response voltage is not exceeded, then the discriminator cannot deliver a pulse. The consequence is that during this time recording is interrupted. The scanning of the field takes place in the vicinity of the emitter in an approximately perpendicular direction. The figures show that at places where the isobars are touched perpendicularly, the record is briefly interrupted.

3.2. The group of two separate emitters

In this section a number of experimentally obtained sound field records are contrasted with graphical representations of calculated fields, as presented by Stenzel and Brosze[8].

In the near field, the group of two individual emitters shows very complex field structure. In the theoretical representation of the field it is necessary to calculate a multiplicity of points in order to be able to review the entire field by interpolation. Moreover it is necessary to carry on a separate calculation for each ratio d/λ (geometrical elongation to the wavelength). Stenzel, therefore, confined himself to a number of specific examples. The graphical representation of the calculated fields is carried out, as for the sound field photograph, by means of curves of constant sound pressure amplitude and equal phase in the plane of the emitter, which is defined by the two emitters and the field points. This type of representation

permits direct comparison between the results of the theoretical calculation and the practical results of measurement in the form of a sound field photograph.

For the calculation of the field it was assumed by Stenzel that the two emitters are of zeroth order, i.e. their dimensions are small compared with the wavelength, and that the distance between the two emitters $d = 2\lambda$. The difference of initial phase between the two emitters is denoted by Ψ, the relationship between the two initial amplitudes by b.

In the practical execution of the comparison two miniature magnetic earphones, which best meet the requirements, were employed as emitters.

So that the sound field photograph could be readily compared with the graphical representation, the phase distribution and amplitude distribution in the field were recorded separately. A frequency of 6.8 kc was chosen for the phase pictures, while the recording of the sound-pressure amplitude was carried out at f = 3.4 kc. Here, owing to the larger distance between emitters ($d = 2\lambda = 20$ cm) a better resolution is obtained, because owing to the interference field the isobars are very close to each other. The enlarged segments were chosen so as to correspond approximately to the scale of Stenzel's sound field representation.

The following case is investigated:

Equal initial amplitude ($b = 1$), same initial phase ($\Psi = 0$)

Sound field record of phase	Figure 9
Sound field record of amplitude	Figure 11
For comparison: (after Stenzel)	
Graphical representation of phase	Figure 10
Graphical representation of amplitude	Figure 12

When we compare the sound field records with the theoretically determined field patterns, good agreement is obtained. However, the following points must be borne in mind:

Stenzel's representations of the lines of constant phase show curves situated closer together than those of the sound field records. In the former case they are drawn with an interval of $\pi/4$, while in the photographs the interval is 2π. There is also a difference in the curves of equal sound pressure amplitude. In the photograph the interval between two lines corresponds to a sound level difference of 5 db, hence gradation conforms to a logarithmic scale. Stenzel, however, shows a linear scale. Here the sound pressure amplitudes 0.25 p, 0.5 p, 0.75 p, 1.0 p, 1.5 p and 2.0 p are assigned to the curves.

It cannot be expected, of course, that the sound field photographs will be entirely similar to the calculated representations, for the same

disturbances (waviness of the isobars) must be expected that were dealt with in the preceding section.

3.3. Investigation of a model bell

3.3.1. Introduction

Having now dealt with sound fields that can easily be grasped, or that have already been calculated, we now consider an emitter whose complete sound propagation conditions have not yet been investigated, namely the bell.

People talk, of course, about the "tone" of a bell. Frequency analysis shows a line spectrum: the tone is made up of various individual tones. Each individual tone of the bell is a certain form of vibration, and is thus associated with a specific sound field.

The first investigations into the vibrational behaviour of the bell were made 100 years ago by H. v. Helmholtz. In his book "The theory of sound sensations"[9], which appeared in 1862, he wrote: "The usual kinds of vibrations (of the bell) are those in which 4, 6, 8, 10 etc. nodal curves form which descend in equal intervals from the crown to the rim."

v. Helmholtz had already recognized the existence of nodal rings: "Other bell vibration forms are also possible, in which nodal circles form that are parallel to the rim; however, these appear difficult to produce and have not yet been investigated."

The optical sound field representation of a model bell is interesting from two points of view. In the first place it gives information concerning the composition of the total sound field from the fields of the individual partial tones. Secondly, it is generally possible without difficulty to draw conclusions concerning the vibrational behaviour of the emitter. The method usually employed hitherto to investigate the individual vibration forms was the point-by-point scanning of the bell surface with vibration pickups.

3.3.2. The recording of the sound fields

When struck with a clapper all individual tones of the bell are excited simultaneously and continue sounding in accordance with their damping. This manner of excitation is not suitable for the photographing of the sound field. We must be certain that the sound field magnitudes remain constant for the entire recording time.

The bell was excited to sinusoidal vibrations by means of an electro-mechanical converter (phonograph record cutting system). It was thus possible to excite the essential partial tones of the bell effectively. These are tones of the following frequencies: 1.4 kc, 3.35 kc, 3.7 kc, 4.7 kc, 6.0 kc, and 9.0 kc.

For each partial tone, three records were made as follows:

1. in a plane parallel to the axis of symmetry of the bell (side view of the bell)*;
2. and 3. in planes perpendicular to the axis of the bell, one below the mouth of the bell (looking down) and the other above the crown (looking up).

In all cases the distance to the object of measurement was made as small as possible, so that from the point of view of the observer the recording plane is immediately behind the bell.

The model bell has a diameter of 177 mm, a height of 142 mm and a weight of 3.2 kg.

3.3.3. Evaluation

The evaluations with respect to the given form of vibration are carried out according to the following scheme:

The plan view of the bell from below gives an idea of the position and number of nodal meridians. These can be determined both from phase and amplitude records. The following is common to all records: in the phase records, radially disposed zones of phase discontinuity can be recognized. They determine the number and position of the nodal meridians. In the region of the phase discontinuity the sound pressure amplitude is 0, while the maximum sound radiation occurs over the vibration bulges. The sound isobars, therefore, yield a pattern characterized by lobes in a stellar arrangement. The number of lobes and their positions determine the vibration bulges. Fig. 13 and Fig. 14 show examples of vibration forms with different numbers of nodal meridians (4,6, 8 and 10).

The sound field records showing the side of the bell yield information on the lateral sound radiation, and thus on the existence of nodal rings (Fig. 15). Here the interpretation is often somewhat more difficult. First it is necessary to realize once more that the sectional plane is situated behind the bell, the lobes which travel radially outward from the bell are thus sectioned.

In general, the sound radiation is such that two main regions may be distinguished. These are the components which are radiated by the vibrating wall of the bell (a) outward and (b) inward (towards the interior of the bell). In view of the field configuration recorded in the plane of the section, these regions must be distinguished. The part of the bell nearest to the scanning plane yields the outwardly radiated component of the sound for

---

* Viewed from the direction of the picture of the suspended bell.

recording purposes. Obviously it is in the vicinity of the radiating surface. The opposite part of the vibrating bell wall also contributes to the field configuration by reason of the component which is radiated towards the interior of the bell. The sound emitted from this part of the bell will be visible in the right-hand part of the records of front of the mouth of the bell.

For the evaluation the record originating from the inwardly radiated sound is of secondary importance. The interesting part of the field lies behind the bell and is in part concealed by it. However, if a nodal ring exists, the sound pressure behind the bell must become 0, in any event along a perpendicular line (Fig. 15b). It must be possible to read this from the position of the isobars in a part not masked by the bell. However, sound field picture Fig. 15a is an example of the case where no nodal ring exists. Here the phase pattern does not play so important a part as the field pictures in the radial plane. The correlation, owing to the different distances between the sectional planes and the radiating parts of the bell, is not always unequivocal.

The individual results thus obtained are summarized in Table IV.

Table IV gives a review of the nodes of the bell vibrations. With increasing frequency a bell vibrates with an ever greater number of subdivided elements. The subdivision is carried out according to certain laws by newly added nodal meridians and rings [10-11].

The very different sound field structure of the individual partial tones emphasizes the known fact that to the ear the bell sounds "dead" whenever the bell itself does not move (for example, the striking of the hour by church steeple clocks). In this case a spectrum is offered to the ear of the observer which varies but slightly. If the bell is tolled, however, the partial tone composition changes continuously at the observer's ear, owing to the fact that because of the sharply differentiated directional characteristics the individual partial tones swell and fade. This makes the sound appear dynamic and alive.

3.4. The sound field of a cylindrical pipe

The sound generated by a hollow cylinder when struck in some respect resembles that of a bell. In geometrical form also there is a relationship between the bell and a short pipe that is closed at one end. It seems obvious therefore, that similarities in the acoustical behaviour will be found.

The following investigations are intended to show that the principal forms of vibration of an open pipe are also characterized by the formation of longitudinal nodal lines (parallel to the longitudinal axis of the pipe) and

nodal rings (perpendicular thereto at the circumference).

The sound emitter was a brass pipe with the following dimensions:

Length 500 mm, outside diameter 90 mm, wall thickness 5 mm.

The pipe was suspended horizontally in two bands of ribbon. As with the bell, the vibrations were excited with the aid of a cutting system in such a way that vibrations are generated in the radial direction. Whereas in the bell that was investigated the number of nodal meridians vary between 4 and 10, only 0 or 1 nodal ring occurs. For the sound field records of the pipe frequencies were selected which also show a greater number of nodal rings:

1. f = 3549 cps, 6 longitudinal nodal lines, 1 nodal ring (Figure 16a);
2. f = 3743 cps, 6 longitudinal nodal lines, 3 nodal rings (Figure 16b);
3. f = 4880 cps, 6 longitudinal nodal lines, 6 nodal rings (Figure 16c).

The sound field records show these conditions very clearly with respect to the nodal rings.

3.5. Sound field records of a violin

Finally, we present sound field records of a violin. Although the representations obtained are scarcely suitable for an evaluation, they are interesting for purposes of comparison with the sound fields hitherto shown. The violin is distinguished as a sound emitter from all other investigated types of emitter, by showing no easily recognizable regularities in its vibrational behaviour.

Again, excitation was brought about with the aid of a phonograph record-cutting system. The needle was located in a small hole in the bridge of the violin. In this manner the violin can be excited to vibration with sinusoidal stresses.

The sound field records (Fig. 17) show a side view of the violin (Meistergeige L. Aschauer, Mittenwald, 1958). Figure 18 shows the section through the field at the level of the bridge.

In Fig. 17a the frequency is f = 3400 cps. In Fig. 17b and 18 f = 5300 cps. These values were selected from the frequency curves of the violin, which shows marked resonance at these points.

It is seen from Fig. 18 that the sound box vibrates in counterphase in the plane of the section. The side view records show that the violin vibrates as an emitter of higher order.

Backhaus[12] and Backhaus and Weymann[13] determined the vibration forms of the sound box for various frequencies by scanning the vibrating surface. They found that a good violin vibrates as an emitter of second order at low frequencies (f ≈ 200 cps) and as one of zeroth order at an intermediate frequency (about f = 270 cps). Within increasing frequency the sound box again

becomes an emitter of higher order. The position and number of nodal lines vary radically with the frequency and also differ on the upper and lower side of the sound box.

From this an extremely complicated field structure results, for which the sound field records are intended to serve as an example.

3.6. Tests in the ultrasonic region

Although the apparatus was not originally intended for frequencies above the audible range, it nevertheless could still be used in the ultrasonic regions (f = 30 kc). For this purpose it is only necessary to use a thinner probe (4 mm diameter). An emitter, whose sound field has been recorded, was built by P. Bocker and was used to generate ultrasound of high intensity in air. The results have already been reported[14].

The investigations were carried out in the Acoustics Section of the Physikalisch-Technische Bundesanstalt. The author wishes to thank Professor Dr. M. Grützmacher, Chief Director of the Department, for encouraging him to do this work and for continually helping with it. Thanks are also due to Dr. W. Kallenbach for many valuable discussions and suggestions.

References

[1] Kock, W. E. und Harvey, F. K., Sound wave and microwave space patterns. Bell Syst. Techn. J. **30** [1951], 564.

[2] Canac, F., Propagation, interférence, réflexion, absorption, diffusion des ondes sonores et ultrasonores visualisées par la méthode de stries. Acustica 4 [1954], 320.

[3] Gavreau, V. et Calaora, A., Enregistrateur automatique de lignes d'égal déphasage. Acustica 6 [1956], 539.

[4] Hübner, G., Die Spiralaustastmethode zur Messung stationärer Schallfelder. Acustica 7 [1957], 191.

[5] Jablonska, H., Eine photographische Methode zur Messung stationärer Schallfelder. Acustica 8 [1958], 63.

[6] Schroeder, H. J., Ein optisches Verfahren zur amplituden- und phasengetreuen Darstellung stationärer Schallfelder. Dissertation TH. Braunschweig 1962.

[7] Grabe, K., Wirkungsweise und Dimensionierung des Schmitt-Diskriminators. Radio-Mentor 6 [1958], 382.

[8] Stenzel, H. und Brosze, O., Leidfaden zur Berechnung von Schallvorgängen. Springer-Verlag, Berlin 1958.

[9] Helmholtz, H. v., Die Lehre von den Tonempfindungen. 6. Aufl. Vieweg und Sohn, Braunschweig 1913.

[10] Grützmacher, M., Über die Klänge von Glocken und Orgeln. Proc. of the I. ICA Congr. Delft 1953, S. 226.

[11] Stüber, C. und Kallenbach, W., Akustische Eigenschaften von Glocken. Phys. Blätter 5 [1949], 268.

[12] Backhaus, H., Über die Schwingungsformen von Geigenkörpern. Z. Phys. 72 [1931], 218.

[13] Backhaus, H. und Weymann, G., Über neuere Ergebnisse der Geigenforschung. Akust. Z. 4 [1939], 302.

[14] Bocker, P., Messungen in Ultraschallfeldern hoher Intensität in Luft. Acustica **11** [1961], 31.

Table I

Decrease of sound level by the 1/r law

Isobar No.	Relative sound level L	Associated sound pressure amplitude p	Associated distance between field points r
	db		
1	0	p_1	17.8 r_6
2	5	1.78 p_1	10.0 r_6
3	10	3.16 p_1	5.6 r_6
4	15	5.6 p_1	3.16 r_6
5	20	10.0 p_1	1.78 r_6
6	25	17.8 p_1	r_6

Table II and Table III
see
Pages 23 and 24

Table IV

Oscillation forms of the model bell

Frequency	Number of nodal lines	Number of nodal rings
kc		
1.4	4	0
3.35	6	0
3.7	4	1
4.7	6	1
6.0	8	0
9.0	10	0

Table II

Evaluation of the sound picture of the spherical emitter (miniature earphone) according to Figure 7

Isobar No.	Assoc. sound level	Max. diam. (Orig. fig.)	Min. diam. (Orig. fig.)	Mean diam. ± dev.	Radius in imaging plane	Dist. between field points $r = \sqrt{a^2 + r'^2}$	Calc. sound level	Mean dev.	Uncertainty (± 0.05 cm in meas.)	Dev. from circ. form (fluct. of level)
	L db	D_{max} cm	D_{min} cm	D_{mean} cm	r' cm	r cm	$L_{calc.}$ db	ΔL db	ΔL db	ΔL db
1	0	7.35	6.65	7.17 ± 0.67	25 ± 2.3	25 ± 2.3	0.9	-0.9	< 0.1	±0.3
2	5	4.4	3.8	4.1 ± 0.3	14.4 ± 1	14.4 ± 1	5.7	-0.7	< 0.1	±0.6
3	10	-	-	2.32	8.15	8.2	10.6	-0.6	< 0.1	-
4	15	-	-	1.33	4.85	4.95	15	±0	±0.2	-
5	20	-	-	0.80	2.8	3.0	19.3	+0.7	±0.4	-
6	25	-	-	0.42	1.47	1.78	23.9	+1.1	±0.7	-

Table III

Evaluation of the sound field picture of the spherical emitter (probe) according to Figure 8

Isobar No.	Assoc. sound level	Max. diam. (Orig. fig.)	Min. diam. (Orig. fig.)	Mean diam. ± dev.	Radius in imaging plane	Dist. between field points $r = \sqrt{a^2 + r'^2}$	Calc. sound level	Mean dev.	Uncertainty (±0.05 cm in meas.)	Dev. from circ. form (fluct. of level)
	L db	D_{max} cm	D_{min} cm	D_{mean} cm	r' cm	r cm	$L_{calc.}$ db	ΔL db	ΔL db	ΔL db
1	0	9.1	7.5	8.25 ± 0.75	23.9 ± 2.6	23.9 ± 2.6	-0.4	+0.4	<0.1	±0.3
2	5	5.1	4.03	4.56 ± 0.53	16.0 ± 1.3	16.0 ± 1.3	4.7	+0.3	<0.1	±0.9
3	10	2.8	2.23	2.54 ± 0.26	8.9 ± 0.9	8.95 ± 0.9	9.8	+0.2	<0.1	±0.3
4	15	1.4	1.35	1.37 ± 0.25	4.8 ± 0.09	4.9 ± 0.09	15.0	±0	±0.2	±0.2
5	20	-	-	0.78	2.72	2.9	19.6	+0.4	±0.4	-
6	25	-	-	0.38	1.35	1.66	24.6	+0.4	±0.7	-

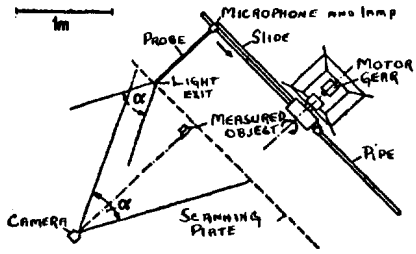

Fig. 1

Ground plane of the experimental set-up in the photography room.

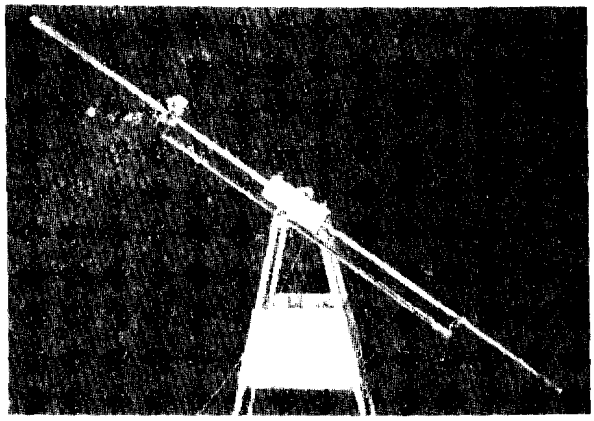

Fig. 2

Scanning apparatus

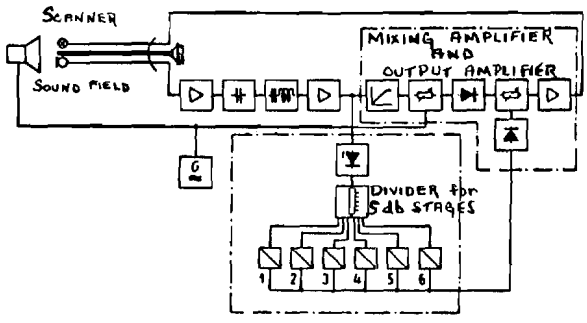

Fig. 3

Block diagram

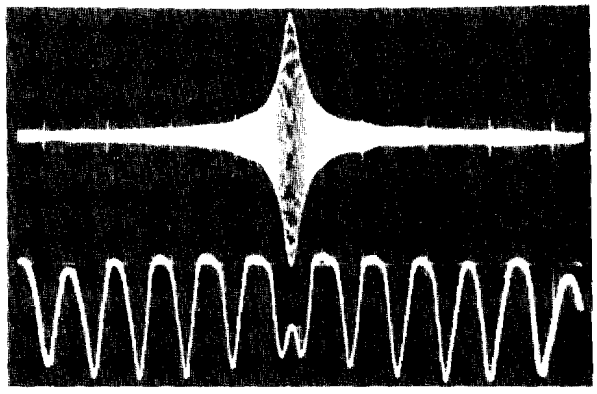

Fig. 4

Oscillogram of the microphone voltage (above) and of the lamp current in phase representation (below). f = 4 kc

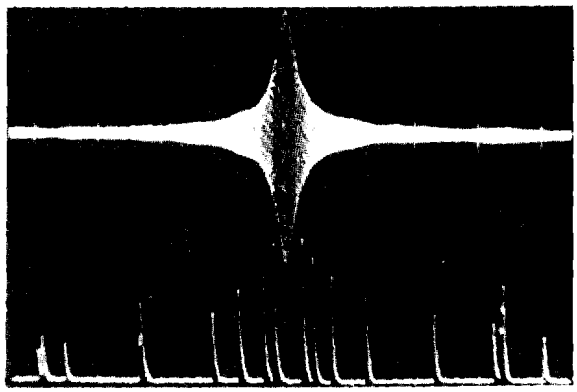

Fig. 5

Oscillogram of the microphone voltage (above) and of the lamp current in amplitude representation (below). f = 4 kc

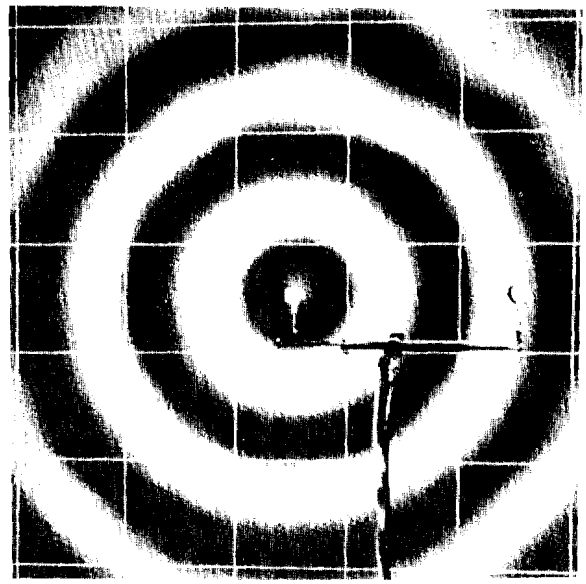

Fig. 6

Sound field of a spherical emitter. Phase representation. f = 3.4 kc

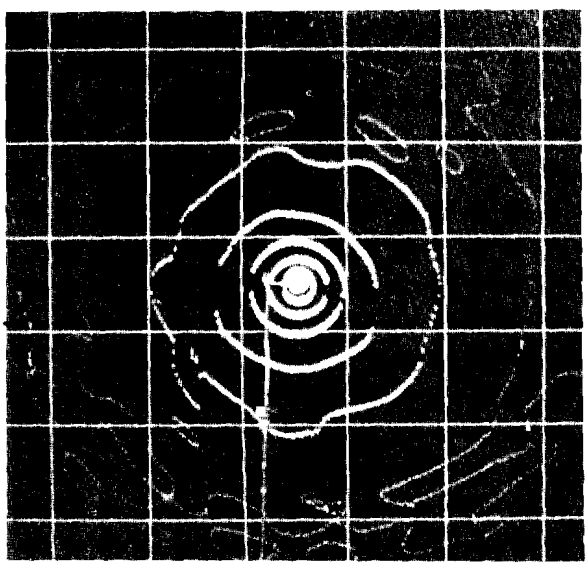

Fig. 7

Sound field of a spherical emitter. Amplitude representation. f = 4 kc. $d/\lambda = 1/4.25$ (d = diameter of emitter)

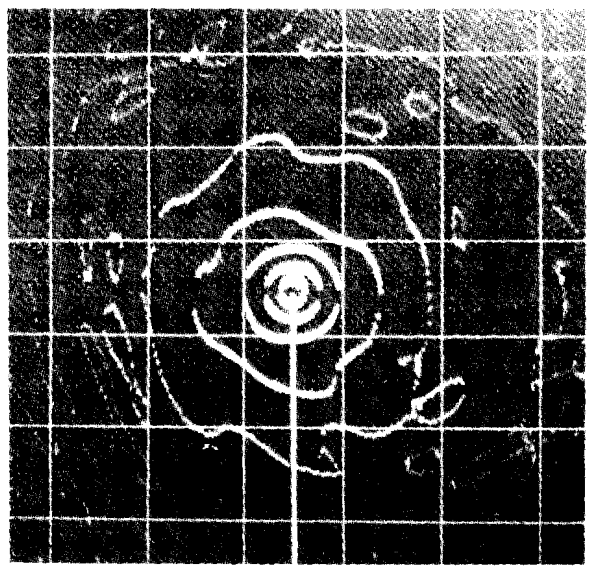

Fig. 8

Sound field of a spherical emitter. Amplitude representation. f = 4 kc. $d/\lambda = 1/14.2$ (d = diameter of emitter)

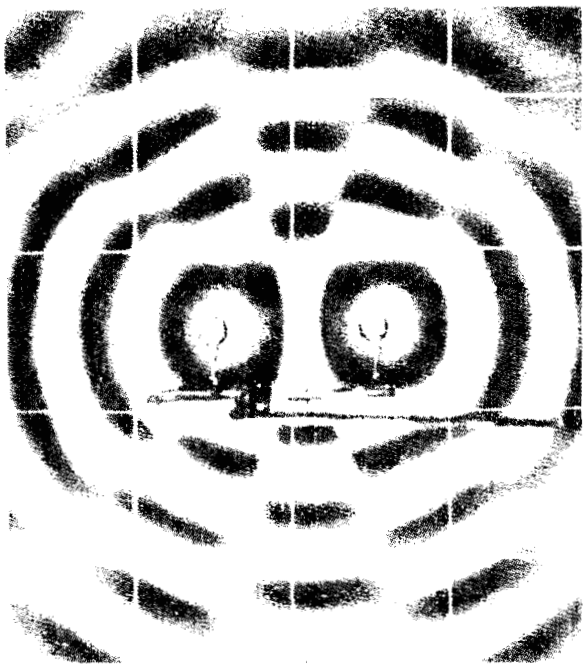

Fig. 9

Sound field of two emitters.
Phase representation.
b = 1; Ψ = 0°; f = 6.8 kc

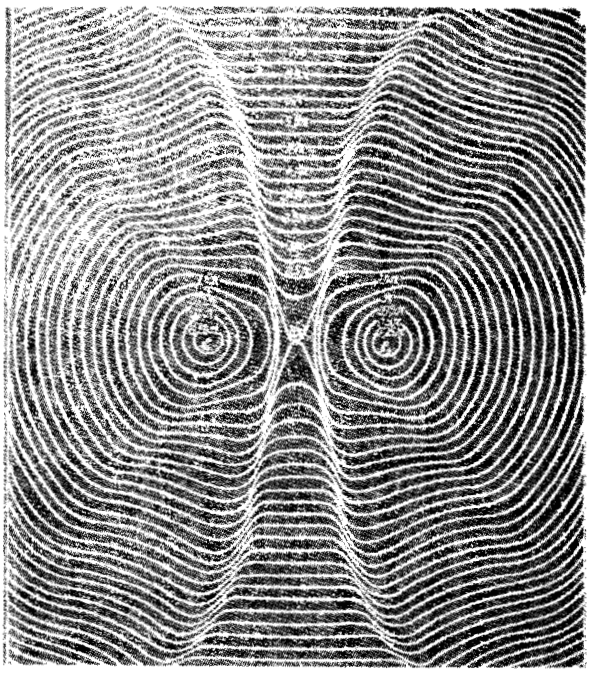

Fig. 10

Sound field of two emitters in graphical representation.
Curves of constant phase.
b = 1; Ψ = 0°. (Taken from ref. 3)

Fig. 11

Sound field of two emitters.
Amplitude representation.
b = 1; Ψ = 0°; f = 3.4 kc

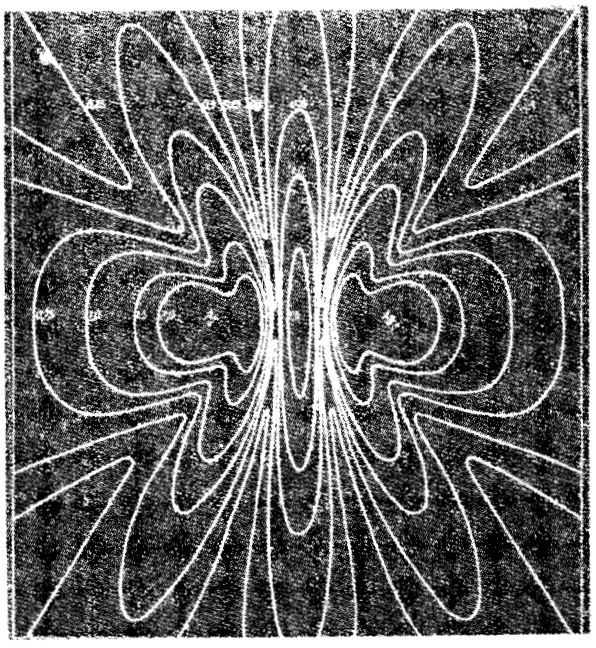

Fig. 12

Sound field of two emitters in graphical representation. Curves of constant sound pressure amplitude.
b = 1; Ψ = 0°. (Taken from ref. 3)

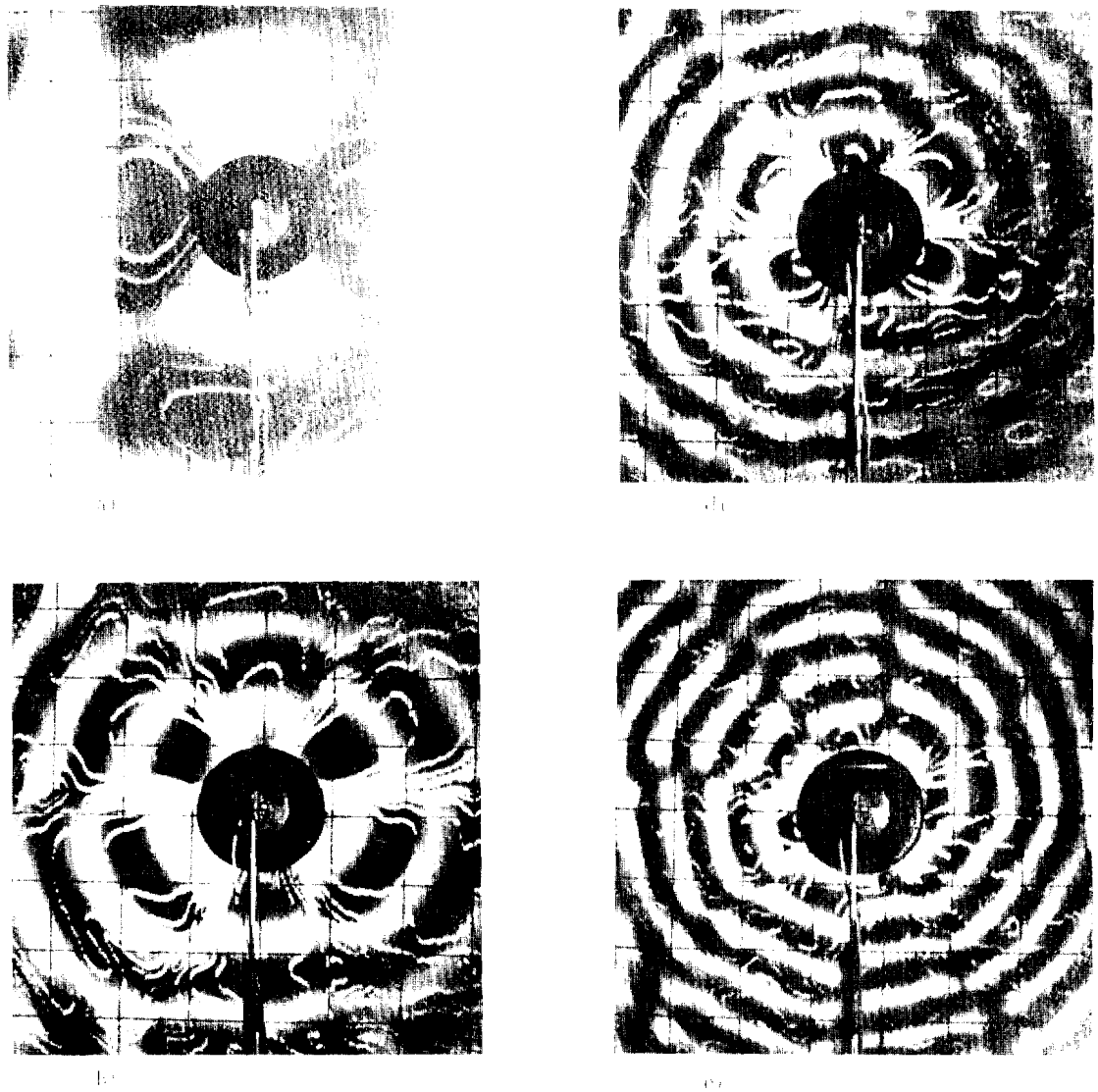

Fig. 13

A model bell excited with various natural vibrations. View from above. Combined phase and amplitude representation. Frequency of partial tones: a) 1.4 kc, b) 3.35 kc, c) 3.7 kc, d) 4.7 kc, e) 6.0 kc

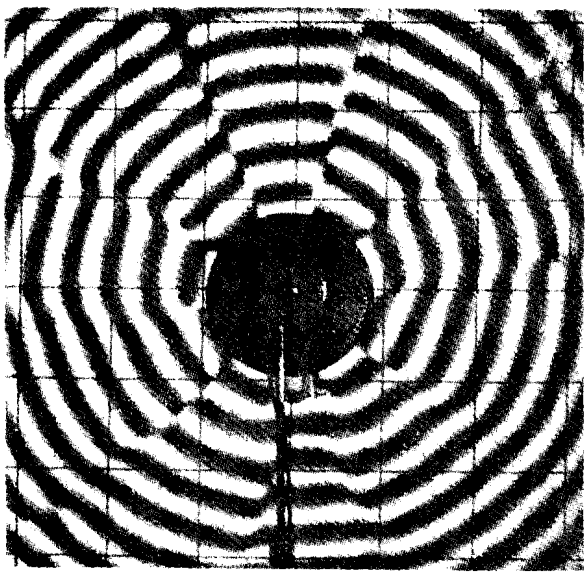

Fig. 14

Sound field of a model bell. View from above. Phase representation. Partial tones: 9.0 kc

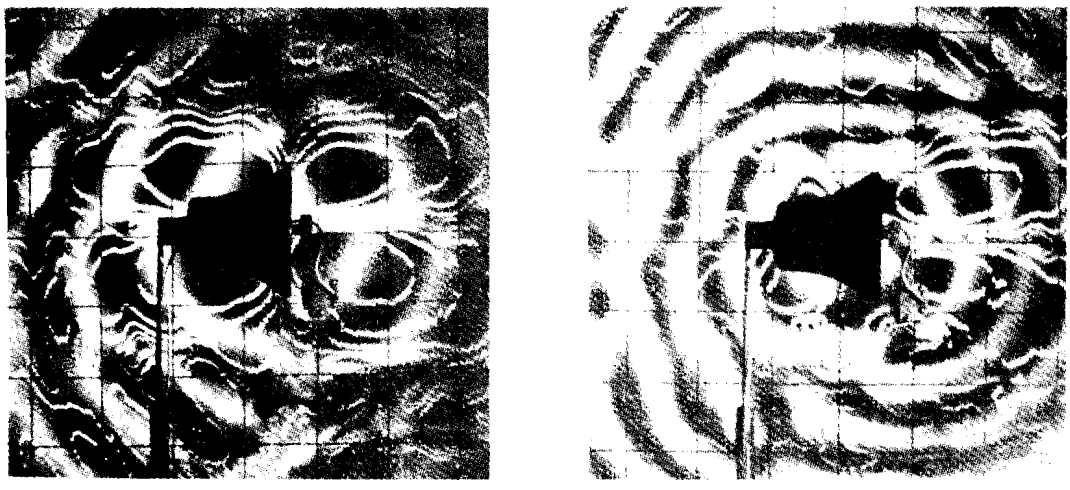

Fig. 15

Sound field of a model bell. Excited to various natural vibrations. Side view. Combined phase and amplitude representation. Frequency of partial tones: a) 3.35 kc, b) 4.7 kc

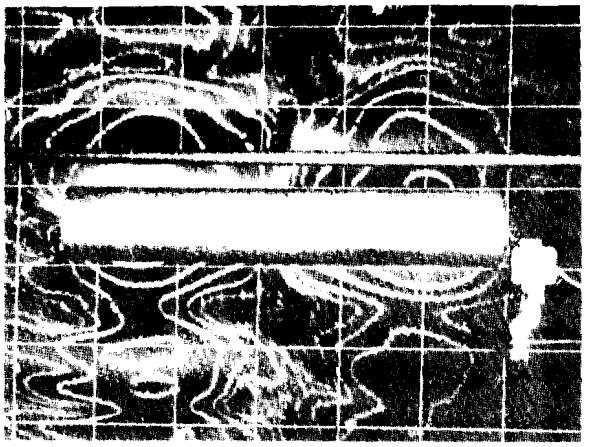

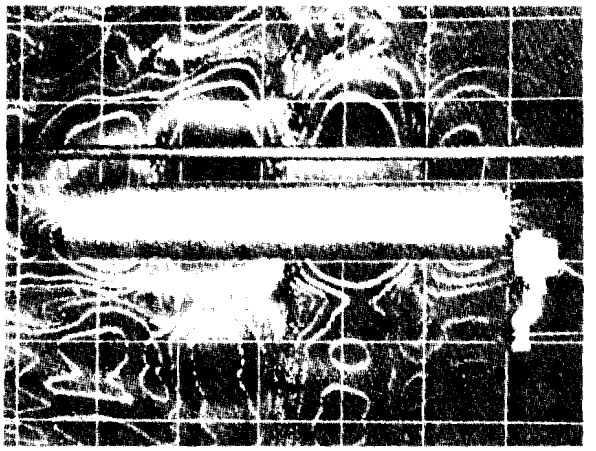

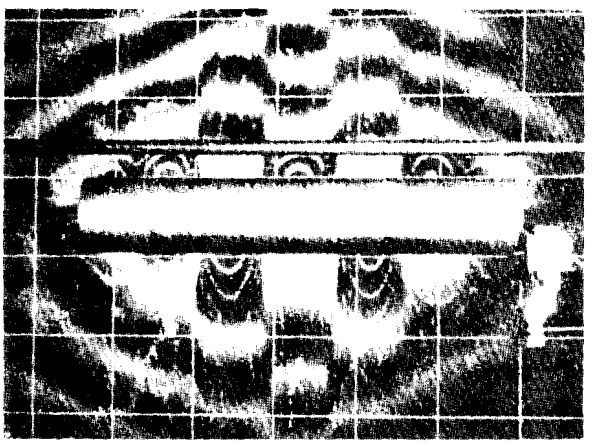

Fig. 16

Sound field of a cylindrical pipe excited to various natural vibrations. Combined phase and amplitude representation. Frequency of partial tones: a) 3.5 kc, b) 3.7 kc, c) 4.9 kc

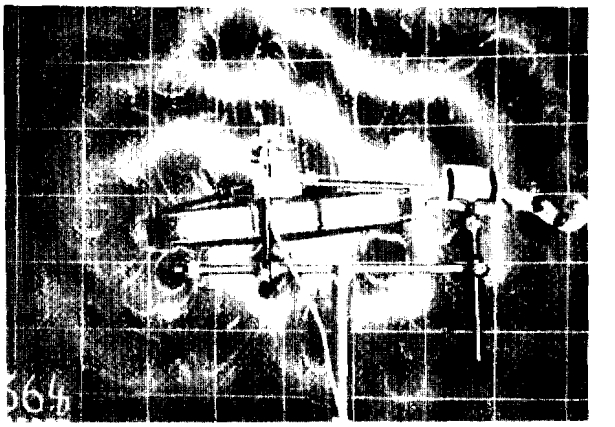

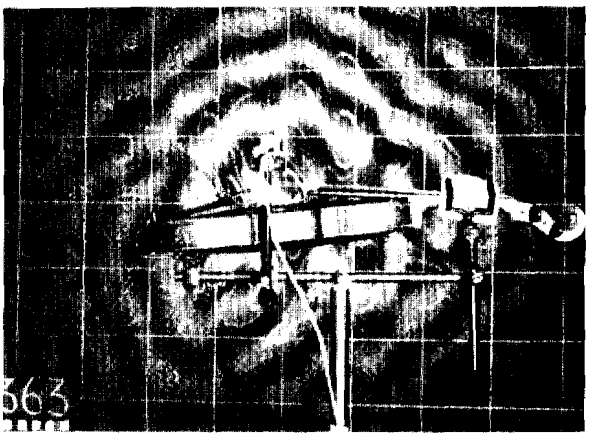

Fig. 17

Sound field of a violin excited with sinusoidal tones. Combined phase and amplitude representation. Side view. Excitation frequency: a) 3.4 kc, b) 5.3 kc

Fig. 18

Sound field of a violin.
Combined phase and amplitude representation.
Section through the field at the level
of the bridge. Excitation frequency 5.3 kc